

MicroRNA-17-5p acts as a biomarker and regulates mitochondrial dynamics in trophoblasts and endothelial cells by targeting the mitofusins Mfn1/Mfn2 in gestational diabetes mellitus

Type

Research paper

Keywords

Biomarker, Gestational diabetes mellitus, MicroRNA-17-5p, Mitofusin, Mitochondrial dynamic

Abstract

Introduction

Gestational diabetes mellitus (GDM) is a metabolic disease that endangers pregnant women and their offspring. Insights into biomarkers and GDM pathogenesis are crucial. Ectopic expression of microRNA-17-5p was found in GDM, but its the diagnostic value and role of miR-17-5p remain unclear.

Material and methods

Detection of miRNA microarray and quantitative PCR (qPCR) found that miR-17-5p was significantly increased and positively associated with biochemical indicators of GDM in 30 GDM plasma samples and 28 matched control plasma samples.

Results

The area under the ROC curve was 0.827 ($P < 0.01$), which showed good diagnostic potential. Mitochondrial staining showed that compared with controls, trophoblasts exhibited more mitochondrial fusion and endothelial cells exhibited more mitochondrial fission in GDM than these in controls. Western blot and qPCR assays further revealed that expression of the mitofusin Mfn1/Mfn2 was lower in primary endothelial cells from GDM patients, whereas their expression was significantly higher in primary trophoblasts from GDM patients compared with those from controls. Conversely, miR-17-5p expression was higher in primary endothelial cells from GDM patients, whereas their expression was significantly lower in primary trophoblasts from GDM patients compared with those from controls. Bioinformatics and luciferase reporter assays confirmed that both Mfn1 and Mfn2 are targets of miR-17-5p. Last, decreased Mfn1/2 was observed not only to increase the apoptotic rate of primary endothelial cells from GDM, but also to reverse anti-apoptotic effects of miR-17-5p inhibitor.

Conclusions

MiR-17-5p regulates Mfn1/Mfn2-mediated mitochondrial dynamics involved in GDM. MiR-17-5p may serve as a promising biomarker and therapeutic target for GDM.

1 **MicroRNA-17-5p acts as a biomarker and regulates mitochondrial**
2 **dynamics in trophoblasts and endothelial cells by targeting the**
3 **mitofusins Mfn1/Mfn2 in gestational diabetes mellitus**

4
5 Jie Li ¹, Zhi-Hui Liu ¹, Tong Wu ², Si Li ³, Ya-nan Sun ^{4*}

6
7 ¹ Department of Obstetrics and Gynecology, Tangshan Gongren Hospital; ² Department of
8 Internal Medicine, Tangshan Gongren Hospital; ³ Department of Cardiology, Tangshan
9 Gongren Hospital; ⁴ Department of Endocrinology, Tangshan Gongren Hospital, Wenhua road
10 27, Tangshan, 063000, Hebei, China.

11
12 *Address for correspondence: Ya-nan Sun, MD, Department of Endocrinology, Tangshan
13 Gongren Hospital, 27 Wenhua Road, Tangshan. E-mail: 826270793@qq.com.

14
15 **Abstract**

16 **Background:** Gestational diabetes mellitus (GDM) is a metabolic disease that endangers
17 pregnant women and their offspring. Insights into biomarkers and GDM pathogenesis are
18 crucial. Ectopic expression of microRNA-17-5p was found in GDM, but its diagnostic value and
19 role of miR-17-5p remain unclear.

20 **Method and result:** Detection of miRNA microarray and qRT-PCR found that miR-17-5p was
21 significantly increased and positively associated with biochemical indicators of GDM in 30
22 GDM plasma samples and 28 matched control plasma samples. The area under the ROC
23 curve was 0.827 ($P < 0.01$), which showed good diagnostic potential. Mitochondrial staining
24 showed that compared with controls, trophoblasts exhibited more mitochondrial fusion and
25 endothelial cells exhibited more mitochondrial fission in GDM than these in controls. Western
26 blot and qRT-PCR assays further revealed that expression of the mitofusin Mfn1/Mfn2 was
27 lower in primary endothelial cells from GDM patients, whereas their expression was
28 significantly higher in primary trophoblasts from GDM patients compared with those from
29 controls. Conversely, miR-17-5p expression was higher in primary endothelial cells from GDM
30 patients, whereas their expression was significantly lower in primary trophoblasts from GDM
31 patients compared with those from controls. Bioinformatics and luciferase reporter assays
32 confirmed that both Mfn1 and Mfn2 are targets of miR-17-5p. Last, decreased Mfn1/2 was
33 observed not only to increase the apoptotic rate of primary endothelial cells from GDM, but
34 also to reverse anti-apoptotic effects of miR-17-5p inhibitor.

35 **Conclusion:** MiR-17-5p regulates Mfn1/Mfn2-mediated mitochondrial dynamics involved in
36 GDM. MiR-17-5p may serve as a promising biomarker and therapeutic target for GDM.

37
38 **Key words:** MicroRNA-17-5p, Biomarker, Mitofusin, Mitochondrial dynamic, Gestational
39 diabetes mellitus

40
41
42
43
44 **Introduction**

45 Gestational diabetes mellitus (GDM), which is characterized by glucose intolerance with
46 onset or first recognition during pregnancy, has become a common health problem worldwide
47 in the context of increased obesity [1]. Its incidence is high in Asians, and its prevalence in
48 China is 14.8% [2]. Unless properly diagnosed and treated, GDM can result in short-term and
49 long-term adverse outcomes for both the mother and fetus, including cesarean section,
50 shoulder dystocia, macrosomia, and neonatal hypoglycemia [3]. Although detection of GDM as
51 early as possible is crucial to avoid poor pregnancy outcomes, the current diagnostic test for
52 GDM is an oral glucose tolerance test (OGTT), which is performed at 24-28 weeks of
53 gestation in compliance with the International Association of Diabetes and Pregnancy Study
54 Groups (IADPSG). Thus, the identification of new biomarkers of GDM is anticipated to predict
55 the early diagnosis of GDM and prevent complications, which is vital to minimize the dangers
56 of hyperglycemia in pregnant women and their children. In addition, in order to find effective
57 therapeutic targets, the pathophysiological mechanism of GDM requires further exploration.

58 Remodeling of the uterine arteries is mediated by extravillous trophoblasts, which
59 penetrate the arterial walls and induce endothelial apoptosis, this is a key event in early
60 pregnancy [4]. Defective remodeling is associated with pregnancy complications, such as
61 preeclampsia and intrauterine growth restriction [5]. The diabetic environment is closely
62 related to endothelial and vascular dysfunction [6], and recently, some miRNAs identified as
63 potential biomarkers of GDM [7] were shown to play an important role in trophoblast-induced
64 endothelial apoptosis [8,9]. Peng et al. reported that high glucose suppresses the viability and
65 proliferation of HTR-8/SVneo cells through regulation of the miR-137/PRKAA1/IL-6 axis [10].
66 Interestingly, literatures reported that mitochondrial fission associated with hyperglycemia
67 induces endothelial cell apoptosis and blood vessel damage [11,12]. Therefore, these findings
68 urged us to explore whether these miRNAs could be the diagnostic, prognostic, and
69 therapeutic targets in GDM.

70 Differential expression of some miRNAs (e.g., miR-17-5p, miR-19a-3p, miR-19b-3p,
71 miR-20a-5p) were found in GDM, suggesting to be potential diagnostic markers [13]. However,
72 opposing miR-17-5p expression patterns between plasma (up-regulation) and placental
73 tissues (down-regulation) [14] from GDM patients implied that further research on the potential
74 molecular mechanisms in GDM is still necessary.

75 Accordingly, in the present study, we studied the expression patterns and diagnostic value
76 of miR-17-5p in a large cohort of GDM patients from the gynaecology and obstetrics
77 departments of Tangshan Gongren Hospital and explored the pathophysiological role of
78 miR-17-5p in trophoblasts and endothelial cells in GDM.

79

80 **Materials and Methods**

81

82 *Clinical specimens*

83 Thirty GDM-complicated pregnancies and 28 normal pregnant women as control were
84 admitted to the gynaecology and obstetrics departments of Tangshan Gongren Hospital
85 between May 2019 and August 2020 were included in this study. Healthy pregnant women as
86 controls not only have normal OGTT, but also meet matched age, body mass index (BMI) and
87 gestational age. The medical history and examination of all enrolled participants should be
88 complete. Of course, patients with GDM who already started oral hypoglycemic drugs, and

89 with history of pre-existing type 1 or 2 DM were excluded. All neonates had a birth weight
90 between the 10th and 90th percentile. None of the women showed signs of hypertension or
91 any other disease. Basic clinical data of the subjects are presented in Table 1. Venous blood
92 samples (5 mL) were centrifuged at $\sim 1,000 \times g$ for 30 min at room temperature, and plasma
93 was stored at -80°C until subsequent analysis. GDM patients were diagnosed by OGTT at 28–
94 32 weeks of gestation as previously described [15]. All patients and controls provided written
95 informed consent. According to the agency guidelines, all these patients had got informed
96 consent before sample collection, and to approve the study by the Research Ethics Committee
97 of XXXXX Hospital (the reference number is GRYY-LL-2019-21).

98

99 *Diagnostic criteria of GDM* [15]

100 The diagnosis of GDM is confirmed using the diagnostic criteria of the IADPSG as
101 followed: fasting plasma glucose (FPG) ≥ 5.1 mmol/L, 1 h PG ≥ 10.0 mmol/L, or 2 h PG ≥ 8.5
102 mmol/L and then undergo a 75 g oral glucose tolerance test (OGTT).

103

104 *miRNA profiling in GDM plasma*

105 Plasma specimens were enrolled from pregnancy (3 women with GDM) and 3 controls
106 matched for maternal age and pregnancy period) **from the gynaecology and obstetrics**
107 **departments of Tangshan Gongren Hospital**. MiRNA extraction and quantification followed a
108 protocol from miRNeasy plasma kit (Qiagen, Hilden, Germany) and an ND-1000
109 spectrophotometer (NanoDrop, Rockland, DE, USA). Further, microRNA-seq was performed
110 on the Illumina HiSeq4000 SE50 (Illumina, San Diego, California, USA) after a miRNA library
111 preparation. Differential miRNA expression analysis was performed using DESeq2 software.

112

113 *Isolation and culture of primary human trophoblasts and endothelial cells*

114 Isolation of primary first-trimester cytotrophoblasts was performed as previously described
115 [16]. Primary human first-trimester decidual ECs were isolated using a modified method
116 described by Grimwood et al [17]. Both primary trophoblasts and endothelial cells were
117 cultured in RPMI1640 culture medium (10% fetal bovine serum) at 37°C , 5% CO_2 , and 95%
118 humidity. Purities of primary trophoblast and endothelial cells were identified by cell
119 immunofluorescence staining using using anti-CK7 (marker for trophoblast cells) and
120 anti-CD31 (marker for endothelial cells) antibodies, respectively. Cell experiment has been
121 approved by the Research Ethics Committee of XXXX Hospital (the reference number is
122 GRYY-LL-2019-21).

123

124 *Transfection of anti-miR-17-5p or si-Mfn1/2 into endothelial cells*

125 ECs in a 6-well plate (2×10^5 cells/well) were maintained in RPMI1640 culture medium (10%
126 fetal bovine serum, 100 U/ml penicillin and 100 $\mu\text{g}/\text{ml}$ streptomycin). For transfection, the
127 anti-miR-17-5p or anti-control (Shanghai Genechem Co., LTD. China) were delivered at a final
128 concentration of 75 nM Lipofectamine® 2000 (Thermo Fisher Scientific, Inc.) following the
129 manufacturer's instructions. Effectiveness of transfection was performed by qRT-PCR to
130 measure the levels of miR-17-5p at 36 h post-transfection.

131

132 Specific small interfering RNA targeting Mfn1 (si-Mfn1) and Mfn2 (si-Mfn2) as well as
corresponding control (si-con) were also purchased from RiboBio. Transfection was conducted

133 using Lipofectamine 2000 (Thermo Fisher Scientific) according to the manufacturer's
134 instructions.

135

136 *Real time quantitative PCR (qRT-PCR)*

137 Total RNA from treated cells and plasma samples was extracted using RNAiso Plus
138 reagent (Takara Bio, Inc.) and TRIzol® LS reagent (Invitrogen; Thermo Fisher Scientific, Inc.),
139 respectively. Then, 0.5 µg total RNA was reverse transcribed into cDNA using a SuperScript®
140 VILO™ cDNA Synthesis Kit and was then used for qRT-PCR with a SYBR Green qPCR Super
141 Mix UDG Kit (Takara Bio, Inc.) according to the corresponding manufacturers' protocols. PCR
142 was performed as follows: 95°C for 2 min followed by 40 cycles at 95°C for 15 s, 60°C for 10 s,
143 and 72°C for 10 s. The relative expression was calculated using the $2^{-\Delta\Delta Ct}$ formula and was
144 normalized to U6, where $\Delta Ct = Ct \text{ related microRNA} - Ct \text{ U6}$ and $\Delta\Delta Ct = \Delta Ct \text{ experimental} - \Delta Ct$
145 control. All PCR was performed in triplicate. The primer sequences of miR-17-5p are as
146 follows: forward 5'-GCCGCCAAAGTGCTTACA-3', reverse, 5'-
147 'CAGAGCAGGGTCCGAGGTA-3'; U6: forward 5'-CTCGCTTCGGCAGCAC-3' and reverse,
148 5'-AACGCTTCACGAATTTGGT-3'.

149

150 *Mitochondrial staining*

151 Mitochondria were visualized with MitoTracker™ Red kit followed the instruction as
152 previously described [18]. Images were captured by confocal microscopy (Nicon Eclipse
153 E-800). The criteria for mitochondrial fission and fusion as followed: when fused, it can form a
154 long rod-shaped, linear and tightly connected three-dimensional mitochondrial network; when
155 it is split, it can form granular, dot-shaped scattered mitochondria.

156

157 *Cell Immunofluorescence*

158 Protocol of cell immunofluorescence staining was described previously [18]. Briefly,
159 primary human trophoblasts and endothelial cells were fixed by Paraformaldehyde (4%) and
160 permeabilized with 0.1% Triton X-100, then blocked with 5% BSA for 1 h, incubated overnight
161 with the primary antibodies anti-cytokeratin-7(CK-7) (1:100, ab68459, Abcam) and anti-CD31
162 (1:100, ab24590, Abcam) at 4°C. Alexa Fluor 568 conjugated secondary antibodies and
163 4'-6-diamidino-2-phenylindole (DAPI) for staining nuclei were employed. Images were viewed
164 by a fluorescent microscope with 400× magnification.

165

166 *Apoptosis assay*

167 Apoptotic rate of endothelial cells was measured using the Annexin-V FITC apoptosis
168 detection kit (Sigma-Aldrich, Merck, Beijing, China). Briefly, primary endothelial cells ($2 \times$
169 10^5 /well) were seeded into 12-well plates and cultured for 48 h at 37°C and then resuspended
170 in HEPES buffer with Annexin-V and PI for detection using flow cytometry (Becton Dickinson,
171 San Jose, CA, USA).

172

173 *Western blot*

174 Western blotting assay was performed as previously described [19]. Briefly, the extracted
175 total protein concentration was determined by a BCA assay. Total protein was separated via
176 SDS-PAGE and then transferred onto PVDF membranes. Non-fat milk for blocking was

177 followed by incubation overnight at 4°C with the following primary antibodies: Anti-Mfn1
178 (1:1,000, 66776-1-Ig, Proteintech); anti-Mfn2 (1:1,000, 67487-1-Ig, Proteintech) and
179 anti-β-actin (1:5,000, 20536-1-AP, Proteintech) and goat anti-rabbit secondary antibodies
180 (SA00001-1, Proteintech). The bonded proteins were visualized by chemiluminescent reaction
181 with ECL (Amersham Pharmacia Biotech, Inc, Little Chalfont, United Kingdom).

182 183 *Luciferase reporter gene*

184 A partial sequence of the 3'-UTRs of Mfn1 and Mfn2 as well as the corresponding mutated
185 miR-17-5p target site in the 3'-UTRs of Mfn1 and Mfn2 were each cloned into the downstream
186 region of the firefly luciferase gene in the pGL2 Vector (Promega, Madison, WI, USA). 293T
187 cells (5×10^4 cells/well) were seeded in 24-well plates and co-transfected with the vector
188 (pGL2-Mfn1-WT or pGL2-Mfn1-MUT and pGL2-Mfn2-WT or pGL2-Mfn2-MUT) and miR-NC
189 mimic or miR-17-5p mimic. After 48 h, the cells were subjected to a dual luciferase assay
190 (Promega, Madison, WI, USA). Detection of the binding ability of miR-17-5p and the Mfn1 or
191 Mfn2 3'-UTRs was performed in three separate experiments. Renilla luciferase activity served
192 as the internal control to normalized luciferase activity.

193 194 *Statistical analysis*

195 SPSS 23.0 software was used for the statistical analyses. Data are presented as means ±
196 standard deviations (SD), and the error bars represent SD. For continuous variables, a
197 comparison between two groups was done using t-test for the normal distribution and
198 Mann-Whitney U test for the non-normal distribution. Correlation test between two continuous
199 variables were done by Pearson correlation coefficient. A receiver operating characteristic
200 (ROC) curve was plotted for miR-17-5p to show the clinical sensitivity and specificity for
201 possible cut-off values. Significance level was $p < 0.05$.

202 203 **Results**

204 205 *Up-regulation of miR-17-5p expression in plasma from women with GDM*

206 Using a high-throughput human miRNA microarray, we found the miRNA expression
207 profiles between 3 GDM plasma specimens and 3 age- and pregnancy-matched normal
208 plasma specimens, which served as corresponding controls. The results of hierarchical
209 clustering and qRT-PCR validation showed top 10 up-regulated miRNAs among the 6 samples
210 (Fig. 1a and 1b).

211 Subsequently, we expanded the sample size (30 GDM specimens: age range from 25 to
212 34, 29.4 ± 3.2 years, and responding 28 control: age range from 24 to 33, 28.9 ± 4.1 years) to
213 confirm increased plasma miR-17-5p expression in GDM. As presented in Fig. 1c, miR-17-5p
214 expression was significantly higher in plasma from GDM patients than that in controls ($P =$
215 0.009). Importantly, the diagnostic value of miR-17-5p in plasma from GDM patients was also
216 verified by ROC curve analysis. The results showed that the area under the ROC curve (AUC)
217 was 0.827 and that the sensitivity and specificity were 0.816 and 0.865, respectively (Fig. 1d).

218 In addition, we also determined whether a high level of miR-17-5p was associated with
219 biochemical parameters of GDM patients. As shown in Table 2, a significant positive
220 correlation was observed between miR-17-5p and FBG, HbA1c, and total cholesterol in GDM

221 patients. These results suggest that miR-17-5p may serve as a promising biomarker for GDM

222

223 *Pattern of mitochondrial dynamics in trophoblasts and endothelial cells*

224 Since the association between mitochondrial fission and endothelial apoptosis has been
225 established in diabetes [20], the mechanism by which the expression of miR-17-5p whether
226 affects trophoblast-induced endothelial cell apoptosis, as mediated by mitochondrial dynamics,
227 was determined by visualizing mitochondrial morphology. Purities of primary trophoblast and
228 endothelial cells were identified by cell Immunofluorescence staining using anti-CK7 and
229 anti-CD31 antibodies, respectively (fig. 2a). The results of MitoTracker™ Red staining showed
230 that most mitochondria in trophoblasts from GDM has a rod-like shape (fused mitochondria). In
231 contrast, in endothelial cells from GDM, increased mitochondrial fission was observed, and the
232 number of endothelial cells containing fragmented mitochondria was much higher in GDM
233 patients than in controls (Fig. 2b and 2c). Furthermore, the mitochondrial fusion-related genes
234 targeted by miR-17-5p were predicted online using TargetScan (Fig. 2d), which implied that
235 the pattern of mitochondrial dynamics (Mitofusins, Mfn1/Mfn2) may play different roles in
236 primary trophoblast and endothelial cells from GDM.

237

238 *Mitochondrial fusion-related Mfn1 and Mfn2 expression is associated with miR-17-5p*

239 To confirm whether Mfn1 and Mfn2 expression is associated with miR-17-5p in different
240 cell types, we detected the expression of these proteins in primary trophoblasts and
241 endothelial cells from GDM and control patients. Western blot and qRT-PCR analysis showed
242 that decreased expression of Mfn1 and Mfn2 as well as increased miR-17-5p expression were
243 observed in endothelial cells from GDM patients compared with controls (Fig. 3a-3b).
244 Conversely, increased Mfn1 and Mfn2 expression as well as decreased miR-17-5p expression
245 were observed in trophoblasts from GDM patients compared with controls (Fig. 3c-3d). To
246 further determine the effect of miR-17-5p knockdown on Mfn1 and Mfn2 expression,
247 endothelial cells were transfected with anti-miR-17-5p, and then qRT-PCR detection for
248 confirming inhibition of its expression (Fig. 3e). Following that, the results of western blot
249 indicated that compared with control, Mfn1 and Mfn2 expression was increased in
250 anti-miR-17-5p-transfected endothelial cells (Fig. 3f). These data suggest that Mfn1 or/and
251 Mfn2 could be target gene of miR-17-5p.

252

253 *Mfn1 and Mfn2 are targets of miR-17-5p*

254 To further explore the relationship between miR-17-5p and Mfn1/Mfn2, the specific binding
255 sites of miR-17-5p in the 3'UTRs of Mfn1 and Mfn2 were predicted by the TargetScan
256 prediction website (Fig. 4a). Moreover, the dual luciferase reporter gene assay was performed
257 to verify the results of bioinformatic prediction (Fig. 4b and 4c). Compared with the negative
258 control (NC) mimic group, luciferase activity was significantly decreased in the miR-17-5p
259 mimic group co-transfected with WT-Mfn1 ($P < 0.05$, Fig. 4b) or WT-Mfn2 ($P < 0.01$, Fig. 4c),
260 while luciferase activity remained unchanged in the miR-17-5p mimic group co-transfected
261 with the MUT-Mfn1 or MUT-Mfn2 plasmid (both $P > 0.05$). These results demonstrated that
262 Mfn1 and Mfn2 are target genes of miR-17-5p.

263

264 *Down-regulation of Mfn1/2 is required for miR-17-5p-mediated cell apoptosis in endothelial*

265 *cells*

266 To examine whether miR-17-5p-mediated apoptotic effects on endothelial cells is
267 Mfn1/2-dependent process, the rescue experiments were performed. We firstly showed the
268 introduction of si- Mfn1/2 for decreased Mfn1 and Mfn2 expression in endothelial cells (Fig. 5a).
269 Subsequently, the results of flow cytometry showed that down-regulation of Mfn1/2 expression
270 promoted cell apoptosis in primary endothelial cells from GDM compared with si-con group;
271 moreover, decreased miR-17-5p exerted anti-apoptotic effect on primary endothelial cells from
272 GDM. Importantly, down-regulation of Mfn1 or Mfn2 expression dramatically reversed the
273 inhibitory effects of anti-miR-17-5p on the apoptosis rate of endothelial cells from GDM (Fig.
274 5b). These results indicated that Mfn1 and Mfn2 are downstream targets of miR-17-5p
275 regulating apoptosis of endothelial cells.

276

277 **Discussion**

278 Trophoblast induction of endothelial cell apoptosis is an important mechanism in spiral
279 artery remodeling in early normal pregnancy [21], but the mechanism in complicated
280 pregnancies, such as in patients with GDM, has yet to be determined. MicroRNAs play a key
281 role in many pathophysiological processes, especially by acting as circulating biomarkers and
282 modulators of the proliferation, migration, invasion, and apoptosis of trophoblasts and
283 endothelial cells [8]. The main objective of this study was to verify the clinical significance and
284 application of circulating miR-17-5p in GDM patients and to elucidate the possible molecular
285 mechanism of miR-17-5p in the regulation of mitochondrial dynamics involved in
286 trophoblast-induced endothelial cell apoptosis. We demonstrated that circulating miR-17-5p is
287 a promising biomarker of GDM since it targets Mfn1/Mfn2-mediated regulation of mitochondrial
288 dynamics. This includes up-regulation of miR-17-5p expression in endothelial cells from GDM
289 patients, which induces mitochondrial fission by decreasing Mfn1/Mfn2 expression, whereas
290 down-regulation of miR-17-5p expression in trophoblasts from GDM patients induces
291 mitochondrial fusion by reversing the inhibitory effects of Mfn1/Mfn2. This leads to acceleration
292 of trophoblast-induced endothelial cell apoptosis in GDM.

293 It is well known that fetal trophoblasts in early pregnancy invade the luminal surfaces of
294 the endothelium and replace the endothelial lining to create high-flow, low-resistance vessels
295 for nutritional demands of the fetus [4]. Previous studies had reported increased miR-17-5p in
296 plasma [13] and decreased expression in placental tissues [14] in GDM patients, which implies
297 that ectopic expression of miR-17-5p in trophoblasts and endothelial cells is involved in
298 aberrant remodeling of the uterine arteries in GDM. At present, the associated mechanism is
299 still lacking, besides up-regulation of miRNA17-5p expression in plasma from GDM women,
300 even at 16–19 weeks of pregnancy is positively correlated with insulin resistance, a risk factor
301 of GDM. Mitochondrial dynamics mediate the regulation of cell proliferation, migration, and
302 apoptosis associated with miRNAs [22,23]. Thus far, less is known about the role of
303 miRNA17-5p in mitochondrial fission and apoptosis between trophoblasts and endothelial cells
304 in GDM patients. In this study, we examined the effect of miR-17-5p ectopic expression on the
305 regulation of mitochondrial dynamics as they relate to invading trophoblasts, which induce
306 endothelial cell apoptosis in GDM. Our results showed that alteration of miR-17-5p expression
307 in different cells facilitates the migration of trophoblasts and apoptosis of endothelial cells in
308 GDM as a result of an imbalance in mitochondrial dynamics. Decreased miR-17-5p promotes

309 more mitochondrial fusion in trophoblasts, while increased miR-17-5p promotes more
310 mitochondrial fission in endothelial cells, which may be a possible mechanism of nutrient
311 oversupply. This in turn leads to macrosomia and other fetal and maternal complications.

312 Offspring born to diabetic mothers are at risk of metabolic diseases associated with
313 mitochondrial dysfunction. Mfn1/Mfn2 are potent modulators of mitochondrial metabolism and
314 insulin signaling and play a key role in mitochondrial dynamics [24,25]. Some literatures
315 indicate that Mfn1 is a major mediator contributing to glucose metabolic
316 reprogramming in cancers [26,27]. Meanwhile, Mfn2 over-expression also leads to
317 cell invasion in lung adenocarcinoma and gastric cancer [28, 29], implying that
318 up-regulation of Mfn1/2 prompting more aggressive in throphoblasts, in turn
319 accelerating the apoptosis of endothelial cells in GDM patients. Notably, a recent study
320 showed that miR-20b suppresses mitochondrial dysfunction-mediated apoptosis to alleviate
321 hyperoxia-induced acute lung injury by directly targeting Mfn1 and Mfn2 [30]. This is in line
322 with our miRNA microarray, which showed up-regulation of miR-20 in plasma from GDM
323 patients. This suggests that up-regulation of both miR-20 and miR-17-5p may play a role in
324 endothelial cell apoptosis induced by excessive oxygen and hyperglycemia. These results
325 presented that miR-17-5p, as a promising biomarker, was selectively expressed in GDM and
326 targets Mfn1/Mfn2-mediated mitochondrial dynamics to intervene different cell type-dependent
327 roles. In addition, recent report showed that miRNAs could manipulate nutrition metabolism,
328 especially glucose and lipid metabolism, by regulating insulin signaling pathways,
329 mitochondrial abnormalities-associated energy metabolism [31], considering the linking
330 between miRNA17-5p-mediated mitochondrial fission and insulin resistance in GDM, prone to
331 hypothesis that miRNA17-5p-mediated nutrition and ATP metabolisms could play a critical role
332 in the pathophysiological mechanism, still deserving further discussion.

333 Overall, our findings provide convincing evidences that miR-17-5p exerts bidirectional
334 regulatory effects on the migration of trophoblasts and the apoptosis of endothelial cells by
335 targeting the expression of the mitofusins Mfn1/Mfn2 in GDM.

336

337 Reference

338

- 339 1. **American Diabetes Association.** Classification and Diagnosis of Diabetes: Standards of
340 Medical Care in Diabetes-2019. Diabetes Care 2019;42:S13-S28.
- 341 2. **Yuen L, Saeedi P, Riaz M, et al.** Projections of the prevalence of hyperglycaemia in
342 pregnancy in 2019 and beyond: results from the International diabetes Federation
343 diabetes atlas, 9th edition. Diabetes Res Clin Pract 2019;157:107841-107861.
- 344 3. **Filardi T, Tavaglione F, Di Stasio M, et al.** Impact of risk factors for gestational diabetes
345 (GDM) on pregnancy outcomes in women with GDM. J Endocrinol Invest
346 2018;41:671-676.
- 347 4. **Jingjing Xu, Haiyi Liu, Yuanyuan Wu, et al.** Proapoptotic effect of metalloproteinase 9
348 secreted by trophoblasts on endothelial cells. J Obstet Gynaecol Res 2011;37(3):187-194.
- 349 5. **Brosens JJ, Pijnenborg R, Brosens IA.** The myometrial junctional zone spiral arteries in
350 normal and abnormal pregnancies: a review of the literature. Am J Obstet Gynecol
351 2002;187:1416-1423.
- 352 6. **Dziedzic EA, Gašior JS, Pawłowski M, et al.** Vitamin D level is associated with severity of

- 353 coronary artery atherosclerosis and incidence of acute coronary syndromes in
354 non-diabetic cardiac patients. *Arch Med Sci* 2019;15(2): 359-368.
- 355 7. **Abdeltawab A, Zaki ME, Abdeldayem Y, et al.** Circulating microRNA-223 and
356 angiopoietin-like protein 8 as biomarkers of gestational diabetes mellitus. *Br J Biomed Sci*
357 2020;61:1-6.
- 358 8. **Liu RH, Meng Q, Shi YP, et al.** Regulatory role of microRNA-320a in the proliferation,
359 migration, invasion, and apoptosis of trophoblasts and endothelial cells by targeting
360 estrogen-related receptor. *J Cell Physiol* 2018;234(1):682-691.
- 361 9. **Ji YT, Zhang WF, Yang J, et al.** MiR-193b inhibits autophagy and apoptosis by targeting
362 IGFBP5 in high glucose-induced trophoblasts. *Placenta* 2020;101:185-193.
- 363 10. **Peng HY, Li MQ, Li HP.** High glucose suppresses the viability and proliferation of HTR
364 8/SVneo cells through regulation of the miR-137/PRKAA1/IL-6 axis. *Int J Mol Med*
365 2018;42:799-810.
- 366 11. **Hao Y, Liu HM, Wei X, et al.** Diallyl trisulfide attenuates hyperglycemia-induced endothelial
367 apoptosis by inhibition of Drp1-mediated mitochondrial fission. *Acta Diabetol*
368 2019;56(11):1177-1189.
- 369 12. **Ma LJ, Zhang ZW, Dong K, et al.** TWIST1 alleviates hypoxia-induced damage of
370 trophoblast cells by inhibiting mitochondrial apoptosis pathway. *Exp Cell Res*
371 2019;385(2):111687-111696.
- 372 13. **Cao YL, Jia YJ, Xing BH, et al.** Plasma microRNA-16-5p,-17-5p and -20a-5p: novel
373 diagnostic biomarkers for gestational diabetes mellitus. *J Obstet Gynaecol Res* 2017;43:
374 974-981.
- 375 14. **Tang L, Li P, Li L.** Whole transcriptome expression profiles in placenta samples from
376 women with gestational diabetes mellitus. *J Diabetes Investig* 2020;11(5):1307-1317.
- 377 15. **Sun DG, Tian S, Zhang L, et al.** The miRNA-29b is downregulated in placenta during
378 gestational diabetes mellitus and may alter placenta development by regulating
379 trophoblast migration and invasion through a HIF3A-dependent mechanism. *Front*
380 *Endocrinol* 2020;11:169-178.
- 381 16. **Cartwright JE, Kenny LC, Dash PR, et al.** Trophoblast invasion of spiral arteries: a novel
382 in vitro model. *Placenta* 2002;23:232-235.
- 383 17. **Grimwood J, Bicknell R, Rees MC.** The isolation, characterization and culture of human
384 decidual endothelium. *Hum Reprod* 1995;10(8):2142-2158.
- 385 18. **Ma D, Zheng B, Liu HL, et al.** Klf5 down-regulation induces vascular senescence through
386 eIF5a depletion and mitochondrial fission. *PLoS Biol* 2020;18(8):e3000808.
- 387 19. **Ma D, Zheng B, Suzuki T, et al.** Inhibition of KLF5-Myo9b-RhoA Pathway-Mediated
388 Podosome Formation in Macrophages Ameliorates Abdominal Aortic Aneurysm. *Circ Res*
389 2017;120(5):799-815.
- 390 20. **Bhatt MP, Lim YC, Kim YM, et al.** C-peptide activates AMPK α and prevents
391 ROS-mediated mitochondrial fission and endothelial apoptosis in diabetes. *Diabetes*
392 2013;62(11):3851-3862.
- 393 21. **Sandra VA, Guy SJW, Philip RD, et al.** Uterine spiral artery remodeling involves
394 endothelial apoptosis induced by extravillous trophoblasts through Fas/FasL interactions.
395 *Arterioscler Thromb Vasc Biol* 2005;25(1):102-118.
- 396 22. **Yan Y, Ma Z, Zhu J, et al.** miR-214 represses mitofusin-2 to promote renal tubular

- 397 apoptosis in ischemic acute kidney injury. *Am J Physiol Renal Physiol*
398 2020;318(4):878-887.
- 399 23. **Channakkar AS, Singh T, Pattnaik B, et al.** MiRNA-137-mediated modulation of
400 mitochondrial dynamics regulates human neural stem cell fate. *Stem Cells*
401 2020;385(5):683-697.
- 402 24. **Gonzalez-Ibanez AM, Ruiz LM, Jensen E, et al.** Erythroid Differentiation and Heme
403 Biosynthesis Are Dependent on a Shift in the Balance of Mitochondrial Fusion and Fission
404 Dynamics. *Front Cell Dev Biol* 2020;8:592035-592049.
- 405 25. **Bruna MG, Thiago SM, Karen FC, et al.** Mice born to females with oocyte-specific
406 deletion of mitofusin 2 have increased weight gain and impaired glucose homeostasis.
407 *Mol Hum Reprod* 2020 26(12):938-952.
- 408 26. **Liu X, Feng C, Wei G, et al.** Mitofusin1 Is a Major Mediator in Glucose-Induced
409 Epithelial-to-Mesenchymal Transition in Lung Adenocarcinoma Cells. *Onco Targets Ther*
410 2020 13: 3511-3523
- 411 27. **Zhang Z, Li TE, Chen M, et al.** MFN1-dependent alteration of mitochondrial dynamics
412 drives hepatocellular carcinoma metastasis by glucose metabolic reprogramming. *Br J*
413 *Cancer* 2020 122(2): 209-220.
- 414 28. **Lou Y, Li R, Liu J, et al.** Mitofusin-2 over-expresses and leads to dysregulation of cell
415 cycle and cell invasion in lung adenocarcinoma. *Med Oncol* 2015 32(4): 132-141.
- 416 29. **Fang CL, Sun DP, Chen HK, et al.** Overexpression of Mitochondrial GTPase MFN2
417 Represents a Negative Prognostic Marker in Human Gastric Cancer and Its Inhibition
418 Exerts Anti-Cancer Effects. *J Cancer* 2017 8(7): 1153-1161.
- 419 30. **Mu G, Deng Y, Lu Z, et al.** miR-20b suppresses mitochondrial dysfunction-mediated
420 apoptosis to alleviate hyperoxia-induced acute lung injury by directly targeting Mfn1 and
421 Mfn2. *Acta Biochim Biophys Sin (Shanghai)* 2020;gmaa161.
- 422 31. **Du H, Zhao Y, Li H, et al.** Roles of MicroRNAs in Glucose and Lipid Metabolism in the
423 Heart. *Front Cardiovasc Med* 2021;8 : 716213-716224.

424

425 **Acknowledgments**

426 We thank Prof. Dong Ma for technical assistance.

427

428 **Author contributions**

429 L. J., L. Z. H., S. Y. N., W. T., L. S., Z. L. C. and O. Y. X. L. performed the experiments and
430 analyzed the data;

431 L. J., S. Y. N. and L. Z. H. conceived and supervised the study; L. J. and S. Y. N. wrote the
432 manuscript.

433

434 **Funding**

435 This work was supported by Medical Science Research Projects of Hebei Provincial Health
436 Commission (No. 20201495).

437

438 **Availability of data and materials**

439 All data produced or analyzed during this study are included in this published article.

440

441 **Declarations**

442 **Ethics approval and consent to participate**

443 Venous blood samples, isolation and culture of primary human trophoblasts and endothelial
444 cells were obtained from patients undergoing surgical resection upon informed consent
445 and approval by the Research Ethics Committee of Tangshan Gongren Hospital (approval
446 number: GRY-LL-2019-21).

447

448 **Consent for publication**

449 Not applicable.

450

451 **Competing interests**

452 The authors state that they have no competing interests.

453

454

455 **Figure legends**

456 **Figure 1 Up-regulation of miR-17-5p expression in the plasma from GDM patients. a,**
457 Hierarchical clustering shows distinguishable miRNA expression (top 10 up-regulated miRNAs)
458 among the 6 samples (3 GDM plasma specimens and 3 age- and pregnancy-matched normal
459 plasma specimens, which served as corresponding controls). **b,** qRT-PCR for verification of
460 different miRNAs expressed in the six samples. *P < 0.05 and **P < 0.01 vs. control, n = 3 for
461 each group. **c,** qRT-PCR to detect the miR-17-5p level in plasma from GDM patients (n = 30)
462 and controls (n = 28). **P < 0.01 vs. control. **d,** Receiver operating characteristic (ROC) curve
463 of circulating miR-17-5p was constructed to predict the diagnostic potential of miR-17-5p for
464 GDM.

465

466 **Figure 2 Mitochondrial dynamics of trophoblasts and endothelial cells. a,** Trophoblasts
467 were derived from primary human first-trimester extravillous trophoblasts, while primary
468 HUVECs were isolated from fresh umbilical cord veins after digestion with collagenase.
469 Representative images of primary trophoblast and endothelial cells purities identified by cell
470 immunofluorescence staining using anti-CK7 (marker for trophoblast cells) and anti-CD31
471 (marker for endothelial cells) antibodies, respectively. Scale bars = 50 μ m. **b,** MitoTracker™
472 Red-stained mitochondria with DAPI for nuclear staining (blue) were observed in primary
473 trophoblasts and endothelial cells from GDM and Control women. Scale bars = 10 μ m. **c,**
474 Statistical analysis for the percentage of cells containing fused and fragmented mitochondria
475 from more than 100 cells between two groups. **P < 0.01 and ***P < 0.001 vs. control, n = 3 for
476 each group. **d,** The miR-17-5p-target regulatory network was constructed based on the
477 TargetScan website (http://www.targetscan.org/vert_72/).

478

479 **Figure 3 Association between abnormal expression of Mfn1, Mfn2, and miR-17-5p in**
480 **trophoblasts and endothelial cells. a,** Western blot for the detection of Mfn1 and Mfn2
481 expression in primary endothelial cells from GDM and control patients. β -actin served as a
482 loading control. **b,** qRT-PCR to detect the miR-17-5p level in primary endothelial cells from
483 GDM and control patients. **P < 0.01 vs. control. **c,** Western blot for the detection of Mfn1 and
484 Mfn2 expression in primary trophoblasts from GDM and control patients. **d,** qRT-PCR to detect

485 the miR-17-5p level in primary trophoblasts from GDM and control patients. *P < 0.05 vs.
486 control. **e**, RT-qPCR for the decreased miR-17-5p expression in anti-miR-17-5p-transfected
487 endothelial cells compared to anti-control-transfected endothelial cells. ***P < 0.001 vs. control.
488 **f**, Western blotting assay for expression of Mfn1, Mfn2 in endothelial cells treated as above.
489 β -actin served as a loading control.

490

491 **Figure 4 MiR-17-5p targets Mfn1 and Mfn2 expression.** **a**, The 3'-UTRs (untranslated
492 regions) sequence for the binding of miR-17-5p to Mfn1/Mfn2. **b** and **c**, 293A cells were
493 transfected with the reporter directed by the Mfn1 and Mfn2 3'UTR containing the miR-17-5p
494 binding site, and luciferase activity was measured. *P < 0.05 and **P < 0.01 vs. NC mimic
495 group.

496

497 **Figure 5 Mfn1/2 expression silencing reverses the anti-apoptosis of miR-17-5p inhibitor**
498 **in primary endothelial cells from GDM.** **a**, The protein level of Mfn1/2 was detected in
499 anti-miR-17-5p-transfected endothelial cells from GDM with Mfn1 and Mfn2 silencing or
500 without by Western blotting assay. **b**, **The apoptosis rates were also analysed in above**
501 **condition by flow cytometry with PI/AnnexinV-FITC. Transfection of anti-control (blue) and anti-**
502 **miR-17-5p (red) in cells indicated different color column.** Data were shown as mean \pm SD, *P <
503 0.05 and **P < 0.01 vs. control or anti-miR-17-5p group.

504

505

506

507

508

509

Table 1 Basic clinical data of the subjects in GDM and Control group

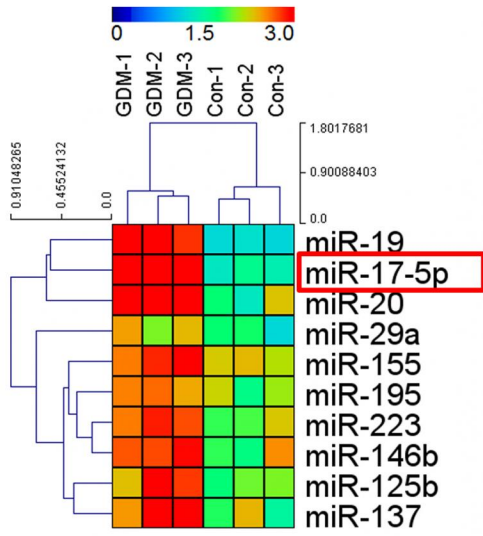
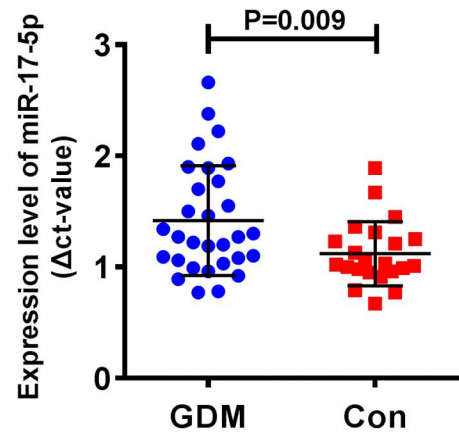
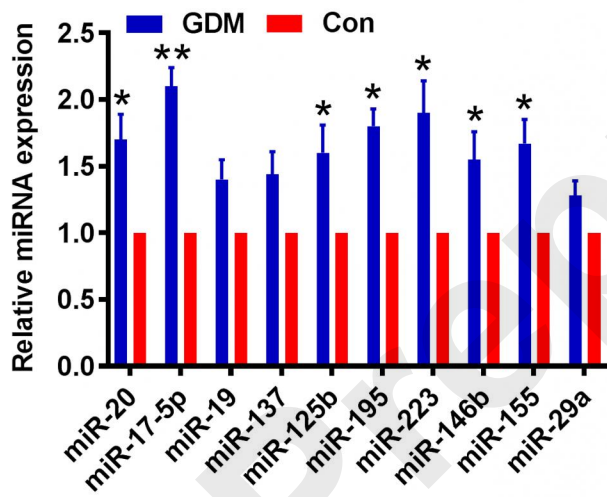
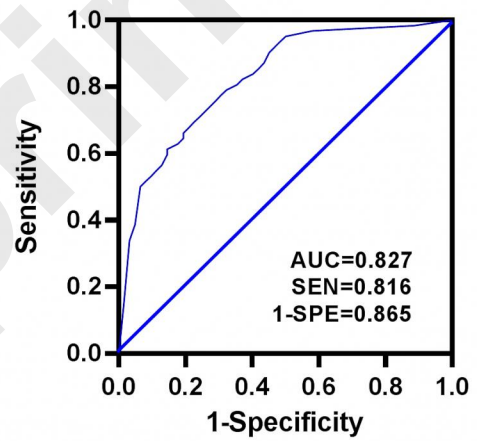
Parameter	GDM (n=30)	Control (n=28)	P value
Age (years)	29.4±3.2	28.9±4.1	0.814
BMI (kg/m ²)	23.8±0.91	23.6±1.08	0.862
FBG (mmol/L)	8.11±1.23	4.85±0.77	<0.001
1h-PPBG (mmol/L)	12.3±1.34	8.94±0.66	<0.001
HbA1c (%)	8.97±1.4	4.17±1.1	<0.001
Total cholesterol (mmol/L)	5.92±1.34	4.33±1.01	<0.01
HDL (mmol/L)	1.22±0.25	1.16±0.21	0.103
LDL (mmol/L)	2.59±0.53	2.77±0.46	0.029
TGs (mmol/L)	2.31±0.68	1.92±0.51	0.087

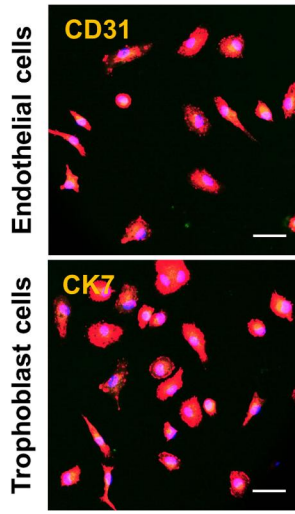
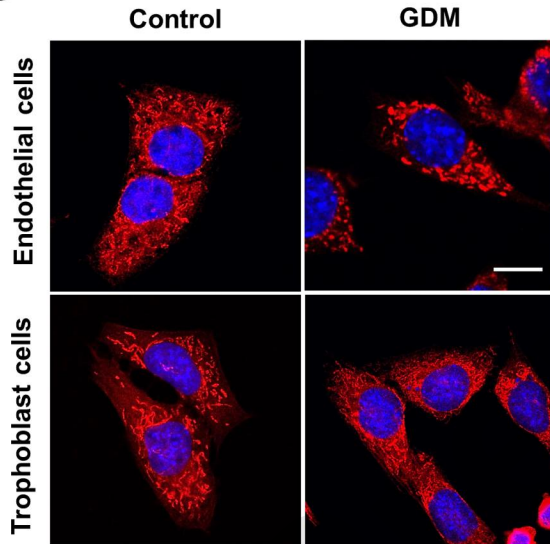
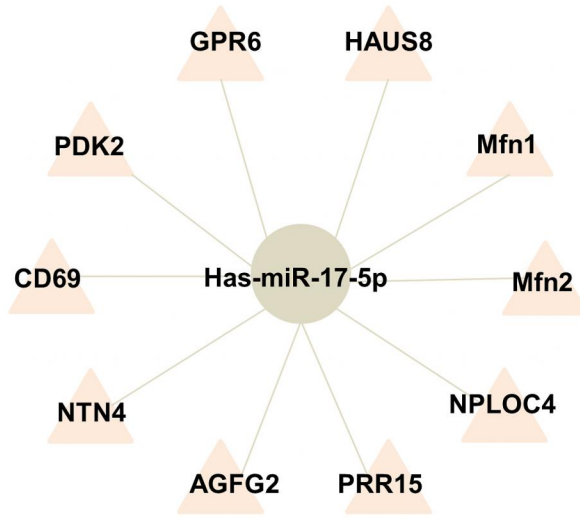
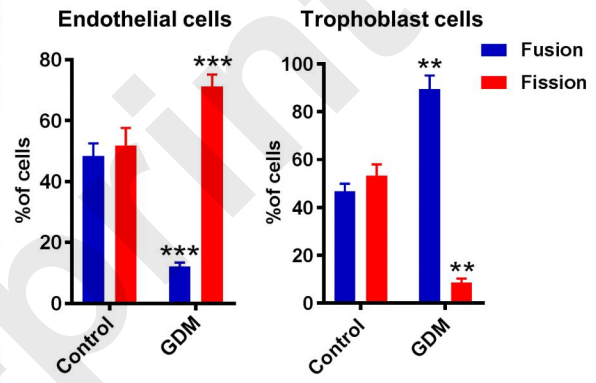
Note: Data was shown as mean ± standard deviation. BMI, body mass index; FBG, fasting blood glucose; PPBG, post-prandial blood glucose; HbA1c, glycated hemoglobin; LDL, low density lipoprotein cholesterol; HDL, high density lipoprotein cholesterol; TGs, triglycerides.

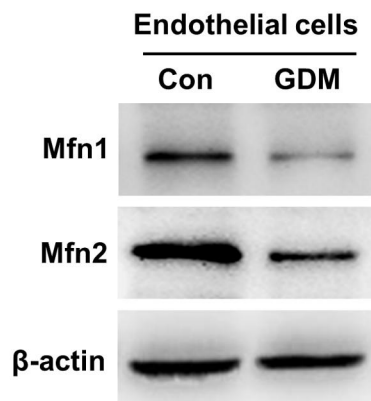
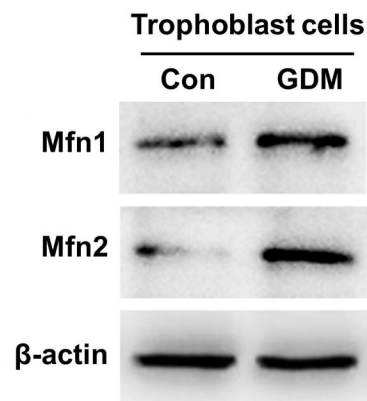
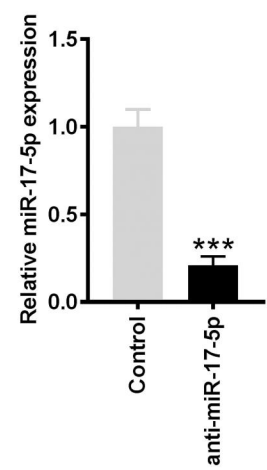
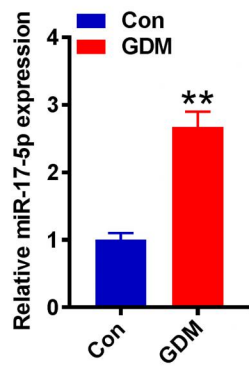
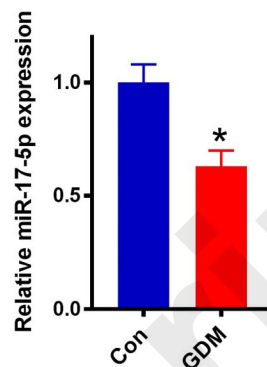
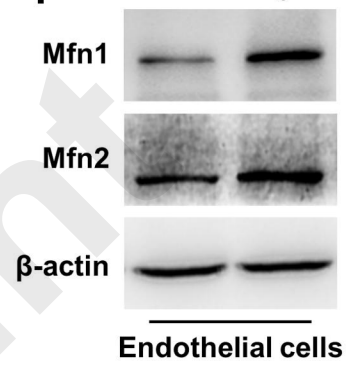
Table 2 Association between miR-17-5p levels and the biochemical parameters in GDM patients

Parameters	FBG	2h-PPBG	HbA1c	Total cholesterol	LDL	HDL	TGs	
miR-17-5p	r	0.473	0.412	0.558	0.486	0.31	-0.16	0.23
	P	<0.001	<0.001	0.007	<0.001	0.023	0.096	0.037

Note: FBG, fasting blood glucose; PPBG, post-prandial blood glucose; HbA1c, glycated hemoglobin; LDL, low density lipoprotein cholesterol; HDL, high density lipoprotein cholesterol; TGs, triglycerides.

A**C****B****D**

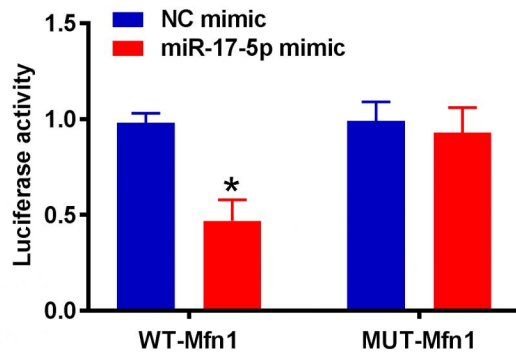
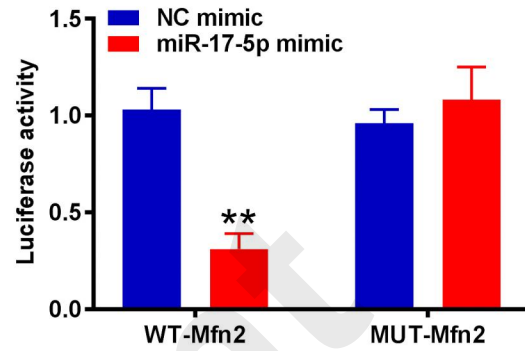
A**B****D****C**

A**C****E****B****D****F**

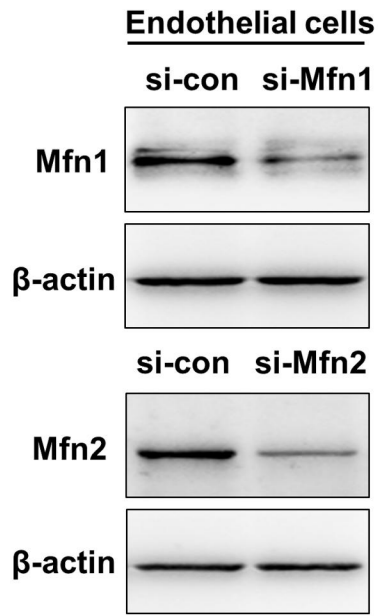
Preprint

A

	Predicted consequential pairing of target region (top) and miRNA (bottom)	Site type	Context++ score
Position 4040-4047 of MFN1 3' UTR	5' ... GAAAUUCUGGUAAAAAGCACUUUA... 	8mer	-0.22
hsa-miR-17-5p	3' GAUGGACGUGACAUCUGUGAAAC		
Position 1775-1782 of MFN2 3' UTR	5' ... GAAGUAUGGCCAAAAGCACUUUA... 	8mer	-0.28
hsa-miR-17-5p	3' GAUGGACGUGACAUCUGUGAAAC		

B**C**

Preprint

A**B**